Eur. Phys. J. Special Topics **145**, 137–157 (2007)

DOI: 10.1140/epjst/e2007-00152-5

THE EUROPEAN PHYSICAL JOURNAL SPECIAL TOPICS

Random waves in the brain: Symmetries and defect generation in the visual cortex

M. Schnabel[1,a], M. Kaschube[1,2], S. Löwel[3], and F. Wolf[1,b]

[1] Max-Planck-Institute for Dynamics and Self-Organization and Bernstein-Center for Computational Neuroscience, Goettingen, Germany
[2] Physics Department and Lewis-Sigler Institute, Princeton University, Princeton NJ, USA
[3] Institute of General Zoology and Animal Physiology, University Jena, Jena, Germany

Abstract. How orientation maps in the visual cortex of the brain develop is a matter of long standing debate. Experimental and theoretical evidence suggests that their development represents an activity-dependent self-organization process. Theoretical analysis [1] exploring this hypothesis predicted that maps at an early developmental stage are realizations of Gaussian random fields exhibiting a rigorous lower bound for their densities of topological defects, called pinwheels. As a consequence, lower pinwheel densities, if observed in adult animals, are predicted to develop through the motion and annihilation of pinwheel pairs. Despite of being valid for a large class of developmental models this result depends on the symmetries of the models and thus of the predicted random field ensembles. In [1] invariance of the orientation map's statistical properties under independent space rotations and orientation shifts was assumed. However, full rotation symmetry appears to be broken by interactions of cortical neurons, e.g. selective couplings between groups of neurons with collinear orientation preferences [2]. A recently proposed new symmetry, called shift-twist symmetry [3], stating that spatial rotations have to occur together with orientation shifts in order to be an appropriate symmetry transformation, is more consistent with this organization. Here we generalize our random field approach to this important symmetry class. We propose a new class of shift-twist symmetric Gaussian random fields and derive the general correlation functions of this ensemble. It turns out that despite strong effects of the shift-twist symmetry on the structure of the correlation functions and on the map layout the lower bound on the pinwheel densities remains unaffected, predicting pinwheel annihilation in systems with low pinwheel densities.

1 Introduction

The ontogenetic development of the cerebral cortex of the brain is a process of astonishing complexity. In every cubic millimeter of cortical tissue in the order of 10^6 neurons must be wired appropriately for their respective functions such as the analysis of sensory inputs, the storage of skills and memory, or motor control [4]. In the brain of an adult animal, each neuron receives input via about 10^4 synapses from neighboring and remote cortical neurons and from subcortical inputs [4]. At the outset of postnatal development, the network is formed only rudimentarily: For instance in the cat's visual cortex, most neurons have just finished the migration from their birth zone lining the cerebral ventricle to the cortical plate at the day of birth [5]. The number of synapses in the tissue is then only 10% and at the time of eye-opening,

[a] e-mail: mick@nld.ds.mpg.de
[b] e-mail: fred@nld.ds.mpg.de

about two weeks later, only 25% of its adult value [6]. In the following 2–3 months the cortical circuitry is substantially expanded and reworked and the individual neurons acquire their final specificities in the processing of visual information [7].

It is a very attractive but still controversial hypothesis that in the ontogenetic development of the brain the emerging cortical organization is constructed by learning mechanisms which are similar to those that enable us to acquire skills and knowledge in later life [8–10]. Several lines of evidence strongly suggest that the brain in a very fundamental sense *learns* to see. First, visual experience is very important for the normal development of sight. If the use of the visual sense is prevented early in life vision becomes irreversibly impaired [7]. Since this is not due to a malformation of the eye or of peripheral stages of the visual pathway, it suggests that in development visual input it used to improve the processing capabilities of the visual cortical networks. In addition, the performance of the developing visual system responds very sensitively to visual experience. In human babies, for instance, already a few hours of visual experience lead to a marked improvement of visual acuity [11]. Second, the synaptic organization of the visual cortex is highly plastic and responds with profound and fast functional and structural reorganization to appropriate experimental manipulations of visual experience [12,13]. These and similar observations suggest that the main origin of perceptual improvement in early development is due to an activity-dependent and thus use-dependent refinement of the cortical network. In the course of this neuronal activity patterns that arise in the processing of visual information in turn guide the further refinement of the cortical network until a mature configuration is reached. Whereas, theoretically, this hypothesis is very attractive, it is, experimentally, still controversial, whether neural activity actually plays such an *instructive* role (for discussion see [14–16]).

Viewed from a dynamical systems perspective, the activity-dependent remodeling of the of the cortical network described above is a process of dynamical pattern formation. In this picture, spontaneous symmetry breaking in the developmental dynamics of the cortical network underlies the emergence of cortical selectivities such as orientation preference [17]. The subsequent convergence of the cortical circuitry towards a mature pattern of selectivities can be viewed as the development towards an attractor of the developmental dynamics [1]. Here we will analyze universal properties of a paradigmatic process in visual cortical development: the development of orientation columns and the formation of their topological defects called orientation pinwheels.

In the visual cortex, as in most areas of the cerebral cortex information is processed in a 2-dimensional (2D) array of functional modules, called cortical columns [18,19]. Individual columns are groups of neurons extending vertically throughout the entire cortical thickness that share many functional properties. Orientation columns in the visual cortex are composed of neurons preferentially responding to visual contours of a particular stimulus orientation [20]. In a plane parallel to the cortical surface, neuronal selectivities vary systematically, so that columns of similar functional properties form highly organized 2D patterns, known as functional cortical maps. In the case of orientation columns, this 2D organization is characterized by so called pinwheels, regions in which columns preferring all possible orientations are organized around a common center in a radial fashion [21,22] (see Figure 1).

Experimental evidence suggests that the formation of orientation columns is a dynamical process guided by neuronal activity and sensitive to visual experience. In normal development, orientation columns first form at about the time of eye opening [23–25]. Comparison of this process to the development under conditions of modified visual experience demonstrates that adequate visual experience is essential for the complete maturation of orientation columns and that impaired visual experience, as with experimentally closed eye-lids can suppress or impair the formation of orientation columns [25]. Most intriguingly, when visual inputs are experimentally redirected to drive what would normally become primary auditory cortex, orientation selective neurons and a pattern of orientation columns even forms in this brain region that would normally not at all be involved in the processing of visual information [26]. In particular the latter observation strongly suggests that the capability to form a system of orientation columns is intrinsic to the learning dynamics of the cerebral cortex given appropriate inputs. Taken

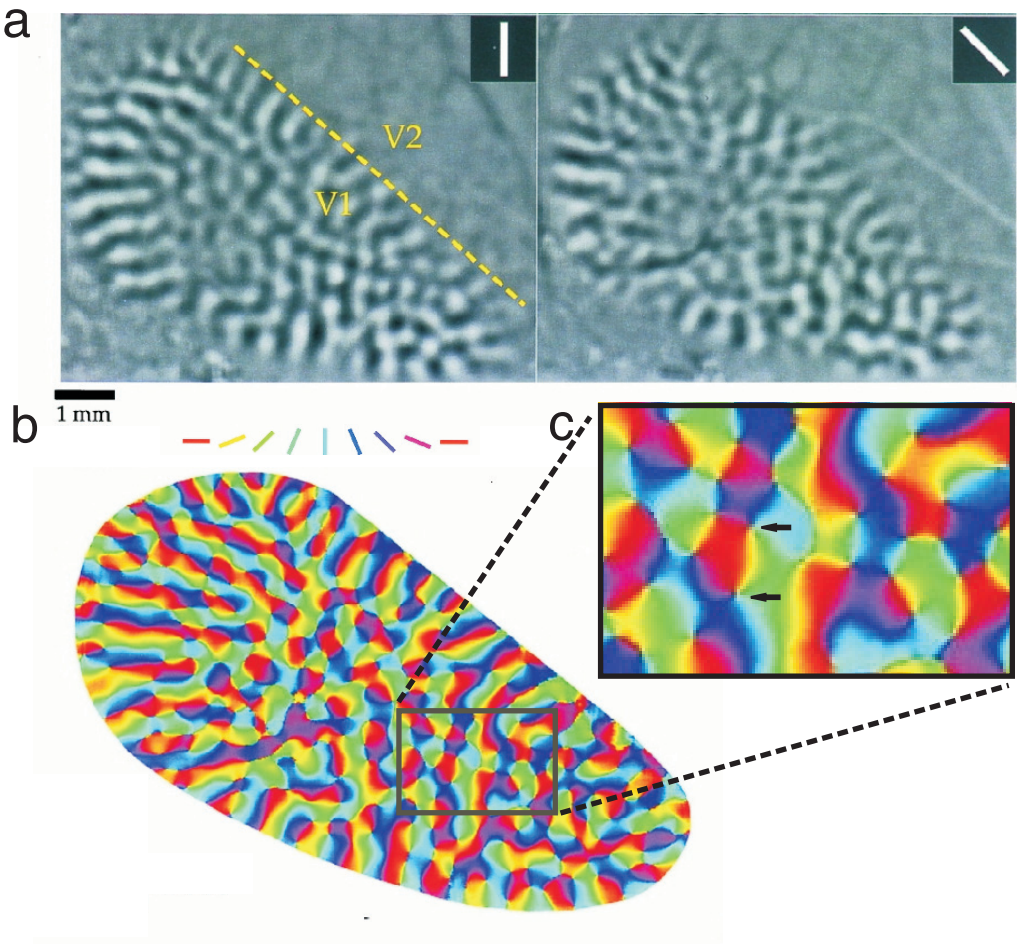

Fig. 1. Patterns of orientation columns in the primary visual cortex of a tree shrew visualized using optical imaging of intrinsic signals (figure modified from [2]). Activity patterns resulting from stimulation with vertically and obliquely oriented gratings are shown in (a). White bars depict the orientation of the visual stimulus. Activated columns are labeled dark grey. The used stimuli activate only columns in the primary visual cortex (V1 in the lower left parts of (a)). The pattern of orientation preferences calculated from such activity patterns is shown in (b). The orientation preferences of the columns are color coded as indicated by the bars. A part of the pattern of orientation preferences is shown at higher magnification in (c). Two pinwheel centers of opposite topological charge are marked by arrows.

together, these lines of evidence mark the formation of orientation columns as a paradigmatic problem in the dynamics of cortical development and plasticity.

Owing to the large number of degrees of freedom of any realistic scale microscopic model of visual cortical development, the description of the development of the pattern of columns by equations for the synaptic connections between individual nerve cells is very complicated. On the order of 10^6 synaptic strengths would be required to realistically describe, for example, the pattern of orientation preference in a $4 \times 4\,\mathrm{mm}^2$ piece of the visual cortex. This complexity and the presently very incomplete knowledge about the nature of realistic equations for the dynamics of visual cortical development demand that theoretical analyzes concentrate on aspects that are relatively independent of the exact form of the equations and are representative for a large class of models. An appropriate framework for this is provided by models in which the emerging cortical architecture is described by order parameter fields and its development by a dynamics of such fields [1,27–33].

A few years ago, Geisel and Wolf discovered that experimentally accessible signatures of an activity-dependent refinement of the cortical network are predicted by universal properties of this very general class of models for the development of visual cortical orientation preference maps [1]. They demonstrated that if the pattern of orientation preferences is set up by learning mechanisms, then the number of pinwheels generated early in development exhibits a universal minimal value that depends only on general symmetry properties of the cortical network. This model suggests that in species exhibiting a lower number of pinwheels in the adult, pinwheels must move and annihilate in pairs during the refinement of the cortical circuitry. Verification of this intriguing prediction would provide striking evidence for the activity-dependent generation of the basic visual cortical processing architecture.

Despite of being valid for a large class of developmental models this result depends on the symmetries of the models and thus of the predicted random field ensembles. In [1] invariance of the orientation map's statistical properties under independent space rotations and orientation shifts was assumed. However, full rotation symmetry appears to be broken by interactions of cortical neurons in V1, e.g. selective couplings between groups of neurons with collinear orientation preferences [2]. A recently proposed new symmetry, called shift-twist symmetry [3], stating that spatial rotations have to occur together with orientation shifts in order to be an appropriate symmetry transformation, is more consistent with this organization.

Here we will analyze the consequences of this reduced symmetry for the generation of pinwheel defects and the layout of orientation maps. Our analysis will be based on the description of the development of orientation preference columns in terms of a dynamics of abstract order parameter fields. We will connect this description to the theory of Gaussian random fields, and show how the theory of Gaussian random fields can be used to obtain quantitative information on the generation and motion of pinwheel defects, in the two dimensional pattern of visual cortical orientation columns. We will also show how the reduced symmetry impacts on the spatial structure of the cortical orientation map.

2 Mathematical framework

2.1 Orientation maps

Orientation preference maps (OPMs) are obtained in optical imaging experiments [22] as follows: The animal's gaze is directed towards a monitor screen where moving oriented bars of a specific orientation θ_n are shown while the cortical activity $E(\mathbf{x}|\theta_n)$ at cortical location $\mathbf{x} = (x, y)$ evoked by this presented stimulus is recorded. The experiment is repeated several times for different orientations θ_n. Standard protocols use $N = 4$, 8 or 16 different orientations, with $\theta_n = n\pi/N$ and index $n = (0, 1, \ldots, N-1)$. In order to obtain the OPM these activity patterns are vector averaged, resulting in a complex valued field,

$$z(\mathbf{x}) = \sum_{n=1}^{N} E(\mathbf{x}|\theta_n) \exp(i\, 2\theta_n)$$

whose argument

$$\theta_{OP}(\mathbf{x}) = \frac{1}{2} \arg\, z(\mathbf{x})$$

then gives the OPM. Experimentally it is found that the activity patterns – therefore also $z(\mathbf{x})$ - are smooth (e.g. [2,**?**,**?**]), in the sense that they change gradually along the cortical surface, without discontinuities. As a result $\theta(\mathbf{x})$ progresses smoothly, too, except at characteristic point-like singularities, called pinwheel centers, located at positions where $z(\mathbf{x}) = 0$.

Our approach in this paper is based on the mathematical description of orientation preference maps in terms of complex valued fields $z(\mathbf{x})$, which we assume to be smooth and sufficiently often differentiable. We adopt the same conventions as in the experiment. Regions where the real (imaginary) part of z prevails, denote regions with horizontal and vertical (right and left oblique) orientation preferences. Retinal coordinates $\mathbf{r}$ are represented in primary visual cortex

coordinates $\mathbf{x}$ by a continuous retinotopic map $\mathbf{r}(\mathbf{x})$. For simplicity we identify cortical and retinal coordinates by setting $\mathbf{r}(\mathbf{x}) = \mathbf{x}$, e.g. the orientation preference with a neuron responding to stimuli at retinal position $\mathbf{r}$ will be represented by $z(\mathbf{r})$.

2.2 Modelling the development of orientation preference maps

We assume that the emergence of OPMs in the visual cortex is caused by activity dependent changes of cortical selectivities driven by afferent activity patterns received from lower stages of the visual pathway. The layout of an OPM $z_{i+1}(\mathbf{x})$ at time $i+1$ after reception of the i-th activity pattern depends on the orientation map at time i, $z_i(\mathbf{x})$, on the retinal input $S(\mathbf{r})$ and on the evoked cortical activity $E(\mathbf{x}) = \mathcal{E}[S(\mathbf{r}), z_i(\mathbf{x})]$ which itself is assumed to be a functional of the retinal input $S(\mathbf{x})$ and the actual orientation map $z_i(\mathbf{x})$, e.g.

$$z_{i+1}(\mathbf{x}) - z_i(\mathbf{x}) = f\left[S, z_i, \mathcal{E}[S, z_i]\right]$$

If the impact of each individual activity pattern is small and afferent activity patterns are randomly drawn from a fixed stimulus ensemble then the temporal evolution of the field $z((x,t))$ on large timescales is described by

$$\partial_t z(\mathbf{x}) = \langle f\left[S, z_i, \mathcal{E}[S, z_i]\right]\rangle_{\{S\}} \tag{1}$$

which does only depend on the stimulus ensemble $\{S\}$ but not on individual stimuli, such that we can write an effective dynamics for $z(\mathbf{x})$ as

$$\partial_t z(\mathbf{x}) = F[z(\mathbf{x})]$$

Clearly $F[z]$ will depend on the statistics of the stimulus ensemble $\{S\}$. For concrete examples of such models see [1] and references therein.

2.3 Symmetry considerations

Models of the form of Eq. (1) can explain the emergence of patterns resembling orientation maps [29,34–36]. Even without specifying the functional form of f, $\mathcal{E}$ and F we can draw some important conclusions on the symmetries they should fullfill. For the following we assume that the stimuli $S(\mathbf{r})$ are assemblies of spatially extended contours, a characteristic feature of natural images, and that the stimulus ensemble $\{S\}$ is rotation, translation and reflection invariant, i.e. for a given $S(\mathbf{r})$ which is in the ensemble also its rotated

$$(\mathbf{R}_\phi S)(\mathbf{r}) := S(\mathcal{R}_\phi^{-1}\mathbf{r}),$$

translated

$$(\mathbf{T}_\mathbf{a} S)(\mathbf{r}) := S(\mathbf{r} - \mathbf{a}),$$

and reflected counterparts

$$(\mathbf{P}S)(x,y) := S(x,-y),$$

are included. A stimulus $S(\mathbf{r})$ will evoke activity in the cortex, denoted by $E(\mathbf{x}) = \mathcal{E}[S,z]$, which also depends on the orientation preference map. Suppose that both, stimulus and orientation preference map are rotated by the same angle ϕ,

$$S' = \mathbf{R}_\phi S \qquad z' = \mathbf{R}_\phi z$$

The evoked response $E = \mathcal{E}[\mathbf{R}_\phi S, \mathbf{R}_\phi z]$ after that rotation will in general be different from the rotated counterpart of E, which we denote by $\mathbf{R}_\phi E$ (see Fig. 2 *left* and *middle column*). However, if together with the spatial rotation of the OPM and the stimulus also the neurons' preferred orientations are shifted by the same angle ϕ,

$$z(\mathbf{x}) \to e^{2i\phi} z(R_\phi^{-1}\mathbf{x}) \equiv e^{2i\phi} R_\phi z$$

then the resulting activity profile will be identical to $\mathbf{R}_\phi E$ (Fig. 2 *right column*),

$$\mathcal{E}[\mathbf{R}_\phi S,\ e^{2i\phi}R_\phi z] = \mathbf{R}_\phi \mathcal{E}[S,\ z].$$

This transformation which couples spatial rotations and shifts in preferred orientation was introduced by Bressloff et al. [3] and called shift-twist transformation (see Fig 2). For the functional f governing activity dependent changes this implies

$$f[\mathbf{R}_\phi S,\ e^{2i\phi}\mathbf{R}_\phi z,\ \mathbf{R}_\phi E] = e^{2i\phi}\mathbf{R}_\phi f[S,\ z,\ E]$$

From these considerations it follows that the effective dynamics $\partial_t z(\mathbf{x}) = F[z(\mathbf{x})]$ must be shift twist equivariant, i.e.

$$\partial_t e^{2i\phi}\mathbf{R}_\phi z = F[e^{2i\phi}\mathbf{R}_\phi z] \stackrel{!}{=} e^{2i\phi}R_\phi F[z]$$

such that shift-twist transformations commute with the functional F and therefore constitute a symmetry of the dynamics:

$$\begin{aligned} F[e^{2i\phi}\mathbf{R}_\phi z] &= \langle f[S,\, e^{2i\phi}\mathbf{R}_\phi z,\, \mathcal{E}[S,\, e^{2i\phi}\mathbf{R}_\phi z]]\rangle_S \\ &= \langle f[\mathbf{R}_\phi S,\, e^{2i\phi}\mathbf{R}_\phi z,\, \mathcal{E}[\mathbf{R}_\phi S,\, e^{2i\phi}\mathbf{R}_\phi z]]\rangle_S = e^{2i\phi}\mathbf{R}_\phi F[z] \end{aligned}$$

Here, the first line is just the definition of the functional F, in the second line we use the rotation invariance of the stimulus ensemble and the last line follows from the properties of the plasticity rule stated above. Similarly from translation and reflection invariant stimulus statistics one obtains equivariance of the dynamics under translations and shift-twist reflections (reflection in coordinate space *and* in preferred orientation)

$$F[\mathbf{T}_\mathbf{a} z] = \mathbf{T}_a F[z] \qquad F[\mathbf{P}\,\bar{z}] = \mathbf{P}\,\overline{F[z]}$$

2.4 Ensembles of orientation preference maps

The layout of an orientation map $z(\mathbf{x},\, t)$ at time t whose development is modeled by a dynamics as in Eq. (1) will depend on the initial conditions $z(\mathbf{x},\, 0)$ at $t = 0$. As suggested by experimental findings the unselective initial state may be modeled by low amplitude random fluctuations of orientation preference. As there is no reason to prefer one initial condition over others the natural approach is to consider an ensemble of OPMs $\{z(\mathbf{x},\, t\}$ consisting of all orientation maps which will evolve out of this set of initial conditions. Statistical properties of such an ensemble are determined by a functional $\mathcal{P}_t[z(\mathbf{x})]$ assigning a statistical weight to each orientation map $z(\mathbf{x})$ in the ensemble at a fixed time t. The dynamics of the ensemble $\{z(\mathbf{x},\, t\}$ is then reflected in the time dependency of the functional $\mathcal{P}_t$. For the early linear (t small) and the asymptotic regimes ($t \to \infty$) one can specify the functional form of $P[z]$. In particular one finds that in the linear regime the ensemble of orientation maps constitutes a Gaussian random field ensemble with Gaussian probability distribution [1,37]. Operations under which the dynamics is equivariant will leave the statistical weight $\mathcal{P}[z]$ invariant and therefore represent a symmetry of the ensemble. In the following we will consider two cases of symmetry classes: Case 1–shift symmetry, denoting symmetry under both, spatial rotations and orientation shifts, applied independently, resulting in a $O(2) \times O(2)$ symmetry group. Case 2 – shift-twist symmetry, denoting symmetry under the reduced $O(2)$ group of shift-twists, where spatial rotations have to occur together with orientation shifts by the same angle. As the degree to which shift symmetry is broken in the visual cortex is currently unknown we will study both cases. In particular, for shift symmetry we have

$$\mathcal{P}[\mathbf{R}_\phi z] = \mathcal{P}[z] \qquad \mathcal{P}[e^{2i\phi}z] = \mathcal{P}[z] \qquad \mathcal{P}[\mathbf{T}_a z] = \mathcal{P}[z] \qquad \mathcal{P}[\mathbf{P}z] = \mathcal{P}[z], \qquad \mathcal{P}[\bar{z}] = \mathcal{P}[z]$$

and for shift-twist symmetry we have

$$\mathcal{P}[e^{2i\phi}\mathbf{R}_\phi z] = \mathcal{P}[z] \qquad \mathcal{P}[\mathbf{T}_a z] = \mathcal{P}[z] \qquad \mathcal{P}[\mathbf{P}\bar{z}] = \mathcal{P}[z]$$

Orientation maps which are related by such a symmetry operation are equivalent in the sense that they will have the same probability of occurring during development.

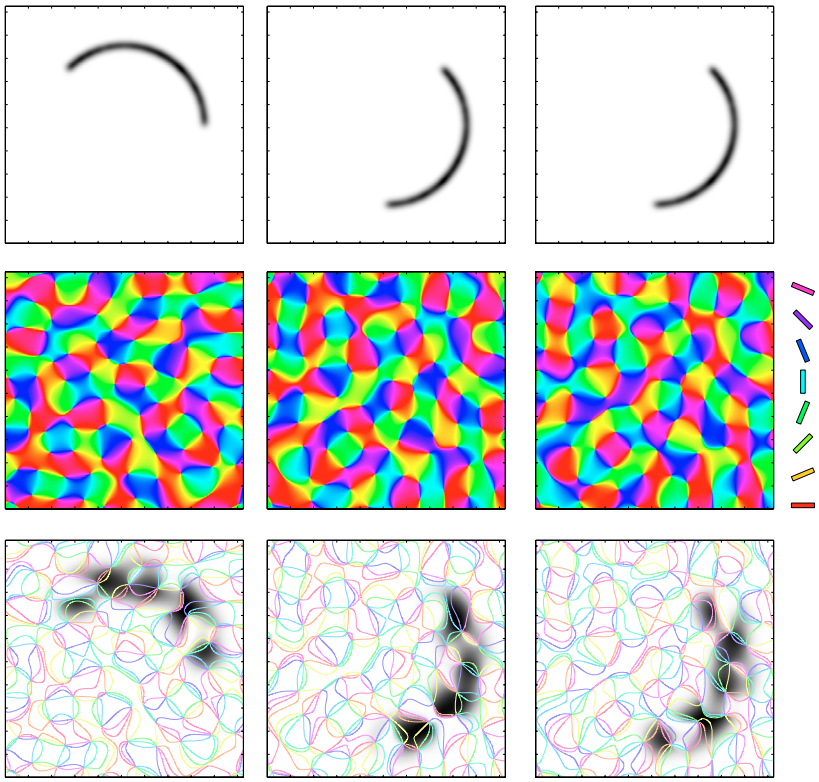

Fig. 2. Scheme illustrating the symmetry of the learning rule under shift-twists. **Left column:** An stimulus, e.g. an elongated contour (*upper left*) elicits an activity profile (*lower left*, active neurons corresponding to dark regions) which depends on the orientation map (*middle left*). **Middle column:** Spatial rotation by an angle ϕ (e.g. here by $\phi = 90°$, clockwise) of the stimulus and the orientation map elicits an activity profile which differs from the rotated profile before. **Right column:** In contrast, the elicited activity profile will be identical to the rotated profile if the OPM is rotated *and* shifted by the same angle at the same time, resulting in a shift-twist rotation.

3 Correlation functions of orientation map ensembles

Given an ensemble within a symmetry class like one of those defined above, what can we tell about the spatial layout of its typical representatives? In this section we will address this issue by analyzing the impact of symmetry assumptions on the form of correlation functions.

3.1 Correlation functions

For any particular point in time the statistical functional $\mathcal{P}_t[z]$ defines an ensemble of random fields at each point in time and thus contains all the information about the ensembles. An equivalent characterization of the ensembles may be given in terms of its correlation functions $c_m^n(\mathbf{x}_1, \mathbf{x}_2, \ldots \mathbf{x}_m, \mathbf{x}_{m+1}, \ldots, \mathbf{x}_{m+n})$ - assuming they exist – defined by

$$c_m^n(\mathbf{x}_1, \mathbf{x}_2, \ldots \mathbf{x}_m, \mathbf{x}_{m+1}, \ldots, \mathbf{x}_{m+n}) = \langle z(\mathbf{x}_1) z(\mathbf{x}_2) \ldots z(\mathbf{x}_m) \bar{z}(\mathbf{x}_{m+1}) \ldots \bar{z}(\mathbf{x}_{m+n}) \rangle$$

where the angular brackets represent the ensemble average. The form of these correlation functions is constrained by the symmetries of the ensemble. Symmetries of the random field ensemble are transformations of the fields $z(\mathbf{x})$ which will leave the functional $\mathcal{P}_t[z]$ and thus also all correlation functions are invariant. For Gaussian random fields, which we will consider subsequently, c_m^n can be expressed by combinations of 1-point and 2-point correlation functions,

such that knowledge of $\langle z(\mathbf{x})\rangle$, $\langle \bar{z}(\mathbf{x})\rangle$,$\langle z(\mathbf{x})\bar{z}(\mathbf{y})\rangle$, $\langle z(\mathbf{x})z(\mathbf{y})\rangle$ provides a complete description of the ensemble. As we assume translation invariance we have

$$\langle z(\mathbf{x})\rangle = \langle z(\mathbf{0})\rangle$$

and the 2-point correlation function such as $\langle z(\mathbf{x}_1)z(\mathbf{x}_2)\rangle$ only depend on their relative argument $\mathbf{r} = \mathbf{x}_2 - \mathbf{x}_1$. We define

$$C_1(\mathbf{r}) = \langle z(\mathbf{x}_1)\bar{z}(\mathbf{x}_1 + \mathbf{r})\rangle \tag{2}$$
$$C_2(\mathbf{r}) = \langle z(\mathbf{x}_1)z(\mathbf{x}_1 + \mathbf{r})\rangle \tag{3}$$

$C_1(\mathbf{r})$ is real, due to translation and inversion symmetry, i.e.

$$C_1(\mathbf{r}) = \langle z(\mathbf{x}_1)\bar{z}(\mathbf{x}_1 + \mathbf{r})\rangle = \langle z(-\mathbf{x}_1 - \mathbf{r})\bar{z}(-\mathbf{x}_1)\rangle = \langle z(\mathbf{x}_1 + \mathbf{r})\bar{z}(\mathbf{x}_1)\rangle = \bar{C}_1(\mathbf{r})$$

and corresponds to the sum of the autocorrelation functions of the real and imaginary parts of $z(\mathbf{x})$, which follows after inserting $z(x) = \mathrm{Re}z(x) + i\,\mathrm{Im}z(x)$,

$$C_1(\mathbf{r}) = \langle \mathrm{Re}z(\mathbf{0})\,\mathrm{Re}z(\mathbf{r})\rangle + \langle \mathrm{Im}z(\mathbf{0})\,\mathrm{Im}z(\mathbf{r})\rangle + i\,\left[\langle \mathrm{Re}z(\mathbf{0})\,\mathrm{Im}z(\mathbf{r})\rangle - \langle \mathrm{Im}z(\mathbf{0})\,\mathrm{Re}z(\mathbf{r})\rangle\right],$$

where the imaginary part vanishes as already shown. $C_2(\mathbf{r})$ is complex, and from

$$\begin{aligned} C_2(\mathbf{r}) &= \langle \mathrm{Re}z(\mathbf{0})\,\mathrm{Re}z(\mathbf{r})\rangle - \langle \mathrm{Im}z(\mathbf{0})\,\mathrm{Im}z(\mathbf{r})\rangle + i\,\left[\langle \mathrm{Re}z(\mathbf{0})\,\mathrm{Im}z(\mathbf{r})\rangle + \langle \mathrm{Im}z(\mathbf{0})\,\mathrm{Re}z(\mathbf{r})\rangle\right] \\ &= \langle \mathrm{Re}z(\mathbf{0})\,\mathrm{Re}z(\mathbf{r})\rangle - \langle \mathrm{Im}z(\mathbf{0})\,\mathrm{Im}z(\mathbf{r})\rangle + 2\,i\,\langle \mathrm{Re}z(\mathbf{0})\,\mathrm{Im}z(\mathbf{r})\rangle \end{aligned}$$

(where again we used translation and inversion symmetry) we see that $\mathrm{Re}C_2(\mathbf{r})$ corresponds to the difference of the autocorrelation functions and $\mathrm{Im}C_2(\mathbf{r})$ to the crosscorrelation of $\mathrm{Re}z(\mathbf{x})$ and $\mathrm{Im}z(\mathbf{x})$.

3.2 Shift-twist symmetry and shift symmetry

We are now prepared to study the additional implications of shift-twist and reflection symmetry on the 2-point functions. Invariance under shift-twist transformations $z(\mathbf{x}) \to \exp(2i\psi)\, z(R_{-\psi}\mathbf{x})$ also implies vanishing of 1-point functions due to the requirement

$$\langle z(\mathbf{0})\rangle \stackrel{!}{=} \exp(2i\psi)\langle z(\mathbf{0})\rangle \quad \forall\psi.$$

In general 2-point correlation functions will not vanish. However, symmetry constrains their functional form. For instance, we will see that $C_2(\mathbf{r})$ is complex valued and can be written in general form

$$C_2(\mathbf{r}) = (x + iy)^4 f(\mathbf{r})$$

with a radially symmetric function $f(\mathbf{r}) = f(|\mathbf{r}|)$. To see this we expand $C_1(\mathbf{r})$ and $C_2(\mathbf{r})$ into power series about $\mathbf{r} = 0$,

$$C_1(\mathbf{r}) = \sum \tilde{a}_{mn}\mathbf{r}^m\bar{\mathbf{r}}^n \tag{4}$$
$$C_2(\mathbf{r}) = \sum \tilde{b}_{mn}\mathbf{r}^m\bar{\mathbf{r}}^n \tag{5}$$

with m, $n \in \mathbb{N}$ and a_{mn}, $b_{mn} \in \mathbb{C}$. Here we identified the coordinate vector $\mathbf{r} = (x, y)$ with the complex number $\mathbf{r} = x + iy$ and performed an expansion in $\mathbf{r}$ and $\bar{\mathbf{r}} = x - iy$, which is strictly equivalent to an expansion in x and y, but has the advantage that spatial rotations $\mathbf{r} \to R_\phi\mathbf{r}$ can be replaced by multiplication with a complex phase $\mathbf{r} \to \exp(i\phi)\mathbf{r}$. Under shift-twist transformations the correlation functions transform as follows:

$$\begin{aligned} C_1(\mathbf{r}) &= \langle z(\mathbf{0})\bar{z}(\mathbf{r})\rangle \to \langle z(\mathbf{0})\,\bar{z}(R_{-\phi}\mathbf{r})\rangle = C_1(R_{-\phi}\mathbf{r}) \\ C_2(\mathbf{r}) &= \langle z(\mathbf{0})\,z(\mathbf{r})\rangle \to e^{4i\phi}\langle z(\mathbf{0})\,z(R_{-\phi}\mathbf{r})\rangle = e^{4i\phi}C_2(R_{-\phi}\mathbf{r}) \end{aligned}$$

Invariance of the correlation functions under shift-twist transformations leads to the conditions

$$C_1(\mathbf{r}) \stackrel{!}{=} C_1(e^{-i\phi}\mathbf{r}) \tag{6}$$

$$C_2(\mathbf{r}) \stackrel{!}{=} e^{4i\phi} C_2(e^{-i\phi}\mathbf{r}) \tag{7}$$

As the left sides of these equations do not depend on ϕ we can average over all angles and obtain

$$C_1(\mathbf{r}) = \sum \tilde{a}_{mn} \mathbf{r}^m \bar{\mathbf{r}}^n \, \frac{1}{2\pi} \int_0^{2\pi} d\phi \, e^{-i\phi(m-n)} = \sum_{n=0}^{\infty} a_n (\mathbf{r}\bar{\mathbf{r}})^n \tag{8}$$

$$C_2(\mathbf{r}) = \sum \tilde{b}_{mn} \mathbf{r}^m \bar{\mathbf{r}}^n \, \frac{1}{2\pi} \int_0^{2\pi} d\phi \, e^{-i\phi(m-n-4)} = (x+iy)^4 \sum_{n=0}^{\infty} b_n (\mathbf{r}\bar{\mathbf{r}})^n \tag{9}$$

from which can read off that $C_1(\mathbf{r})$ is radially symmetric as it only depends on $\mathbf{r}\bar{\mathbf{r}} = x^2 + y^2$. As shown before, $C_1(\mathbf{r})$ is real, and therefore $a_n \in \mathbb{R}$. Furthermore, symmetry under shift-twist reflection $z(x) \to z(\bar{x})$, $z(\mathbf{r}) \to \bar{z}(\bar{\mathbf{r}})$ requires $C_2(\mathbf{r}) = \bar{C}_2(\bar{r})$. This is fullfilled if $b_n \in \mathbb{R}$. Together we get

$$C_2(\mathbf{r}) = (x+iy)^4 f(\mathbf{r}) = \left(x^4 - 6x^2y^2 + y^4 + 4\,i\,xy(x^2-y^2)\right) f(\mathbf{r}) \tag{10}$$

with real, radially symmetric function $f(\mathbf{r}) = \sum_{n=0}^{\infty} b_n (\mathbf{r}\bar{\mathbf{r}})^n$. For $f(\mathbf{r}) \equiv 0$, full $O(2) \times O(2)$ symmetry is restored. In that case $\mathrm{Re}z(x)$ and $\mathrm{Im}z(x)$ are uncorrelated and their autocorrelation functions are identical. However, in general $f(\mathbf{r})$ does not vanish and $O(2) \times O(2)$ symmetry is broken down to the $O(2)$ subgroup of shift-twist transformations.

3.3 Correlation functions in k-space

Alternatively, the 2-point coorelations may also be represented in Fourier representation. The cross correlations of the Fourier modes $a(\mathbf{k}) = \frac{1}{2\pi} \int d\mathbf{k}\, z(\mathbf{x}) e^{-i\mathbf{kx}}$ are given by

$$\langle a(\mathbf{k})\, \bar{a}(\mathbf{k}') \rangle = \frac{1}{(2\pi)^2} \int d\mathbf{x} \int d\mathbf{x}' e^{-i\mathbf{kx}} e^{i\mathbf{k}'\mathbf{x}'} \langle z(\mathbf{x}) \bar{z}(\mathbf{x}') \rangle \tag{11}$$

$$= \frac{1}{(2\pi)^2} \int d\mathbf{x} \int d\mathbf{x}' e^{-i\mathbf{kx}} e^{i\mathbf{k}'\mathbf{x}'} \langle z(\mathbf{0}) \bar{z}(\mathbf{x}' - \mathbf{x}) \rangle \tag{12}$$

$$= \frac{1}{(2\pi)^2} \int d\mathbf{x} \int d\mathbf{x}' e^{i(\mathbf{k}'-\mathbf{k})\mathbf{x}} e^{i\mathbf{k}'\mathbf{x}'} \langle z(\mathbf{0}) \bar{z}(\mathbf{x}') \rangle \tag{13}$$

$$= P_1(\mathbf{k}) \delta(\mathbf{k} - \mathbf{k}') \tag{14}$$

$$\langle a(\mathbf{k})\, a(\mathbf{k}') \rangle = \frac{1}{(2\pi)^2} \int d\mathbf{x} \int d\mathbf{x}' e^{-i\mathbf{kx}} e^{-i\mathbf{k}'\mathbf{x}'} \langle z(\mathbf{x}) z(\mathbf{x}') \rangle \tag{15}$$

$$= \frac{1}{(2\pi)^2} \int d\mathbf{x} \int d\mathbf{x}' e^{-i\mathbf{kx}} e^{-i\mathbf{k}'\mathbf{x}'} \langle z(\mathbf{0}) z(\mathbf{x}' - \mathbf{x}) \rangle \tag{16}$$

$$= \frac{1}{(2\pi)^2} \int d\mathbf{x} \int d\mathbf{x}' e^{-i(\mathbf{k}+\mathbf{k}')\mathbf{x}} e^{-i\mathbf{k}'\mathbf{x}'} \langle z(\mathbf{0}) z(\mathbf{x}') \rangle \tag{17}$$

$$= P_2(\mathbf{k}) \delta(\mathbf{k} + \mathbf{k}') \tag{18}$$

where $P_1(\mathbf{k})$ and $P_2(\mathbf{k})$ denote the Fourier transforms of $C_1(\mathbf{r})$ and $C_2(\mathbf{r})$. From these expressions we see that almost all correlators vanish, except of $\langle a(\mathbf{k})\bar{a}(\mathbf{k})\rangle$ and $\langle a(\mathbf{k})a(-\mathbf{k})\rangle$. Let us briefly note the constraints imposed on $P_1(\mathbf{k})$ and $P_2(\mathbf{k})$ by $O(2) \times O(2)$ and shift-twist symmetry.

1. Invariance of $P_1(\mathbf{k})$ and $P_2(\mathbf{k})$ under coordinate rotations, $a(\mathbf{k}) \rightarrow a(R_\phi^{-1}\mathbf{k})$, reflections, $a(\mathbf{k}) \rightarrow a(\pm\bar{\mathbf{k}})$, orientation shifts, $a(\mathbf{k}) \rightarrow \exp(i\psi)a(\mathbf{k})$ and orientation reflections $a(\mathbf{k}) \rightarrow \bar{a}(\mathbf{k})$ implies rotation invariant, positive $P_1(\mathbf{k})$ and vanishing of $P_2(\mathbf{k})$, such that all Fourier modes decouple:

$$P_1(\mathbf{k}) = \langle a(\mathbf{k})\bar{a}(\mathbf{k})\rangle \stackrel{Rot}{\longrightarrow} \langle a(R_{-\psi}\mathbf{k})\bar{a}(R_{-\psi}\mathbf{k})\rangle = P_1(R_{-\psi}\mathbf{k})$$

$$P_2(\mathbf{k}) = \langle a(\mathbf{k})a(-\mathbf{k})\rangle \stackrel{Shift}{\longrightarrow} \exp 2i\psi\langle a(\mathbf{k})a(-\mathbf{k})\rangle = \exp 2i\psi P_2(\mathbf{k})$$

2. Invariance under shift-twist rotations $a(\mathbf{k}) \rightarrow e^{i2\phi}a(R_\phi^{-1}\mathbf{k})$ and shift-twist reflections $a(\mathbf{k}) \rightarrow \bar{a}(\pm\bar{\mathbf{k}})$ implies rotation invariant, real valued $P_1(\mathbf{k})$ and $P_2(\mathbf{k})$ of the following general form

$$P_2(\mathbf{k}) = \exp(4i\arg(\mathbf{k}))g(\mathbf{k}) \tag{19}$$

with $\arg(\mathbf{k}) := \arg(k_x + ik_y)$ and rotation invariant, real valued $g(\mathbf{k})$:

$$P_1(\mathbf{k}) = \langle a(\mathbf{k})\bar{a}(\mathbf{k})\rangle \stackrel{ShTw}{\longrightarrow} \langle a(R_{-\phi}\mathbf{k})\bar{a}(R_{-\phi}\mathbf{k})\rangle = P_1(R_{-\phi}\mathbf{k})$$

$$P_2(\mathbf{k}) = \langle a(\mathbf{k})a(-\mathbf{k})\rangle \stackrel{ShTw}{\longrightarrow} \exp(4i\phi)\langle a(R_{-\phi}\mathbf{k})a(-R_{-\phi}\mathbf{k})\rangle = \exp(4i\phi)P_2(R_{-\phi}\mathbf{k})$$

Any function $P_2(\mathbf{k})$ fullfilling this condition is of the form

$$P_2(\mathbf{k}) = \exp(4i\arg(\mathbf{k}))g(\mathbf{k}).$$

Invariance under shift-twist reflections finally requires

$$g(\mathbf{k}) = \bar{g}(\mathbf{k})$$

such that $g(\mathbf{k}) \in \mathbb{R}$.

3.4 The degree of shift-symmetry breaking

From this follows that the covariance matrix C of

$$\boldsymbol{\eta}(\mathbf{k}) := (\mathrm{Re}a(\mathbf{k}),\ \mathrm{Re}a(-\mathbf{k}),\ \mathrm{Im}a(\mathbf{k}),\ \mathrm{Im}a(-\mathbf{k}))$$

is

$$\mathsf{C}(\mathbf{k}) = \frac{1}{2}\begin{pmatrix} P_1(\mathbf{k}) & \mathrm{Re}P_2(\mathbf{k}) & 0 & \mathrm{Im}P_2(\mathbf{k}) \\ \mathrm{Re}P_2(\mathbf{k}) & P_1(\mathbf{k}) & \mathrm{Im}P_2(\mathbf{k}) & 0 \\ 0 & \mathrm{Im}P_2(\mathbf{k}) & P_1(\mathbf{k}) & -\mathrm{Re}P_2(\mathbf{k}) \\ \mathrm{Im}P_2(\mathbf{k}) & 0 & -\mathrm{Re}P_2(\mathbf{k}) & P_1(\mathbf{k}) \end{pmatrix}. \tag{20}$$

It has two eigenvalues

$$\lambda_{1,2}(\mathbf{k}) = \frac{1}{2}\left[P_1(\mathbf{k}) \pm |P_2(\mathbf{k})|\right], \tag{21}$$

each of which is doubly degenerated. Since a covariance matrix is positive definite, $P_1(\mathbf{k})$ and $P_2(\mathbf{k})$ must satisfy the inequality

$$|P_2(\mathbf{k})| \leq P_1(\mathbf{k}). \tag{22}$$

for any admissible pair of correlation functions. A convenient measure of the degree of shift symmetry breaking is derived from the ratio

$$Q(\mathbf{k}) := \frac{|P_2(\mathbf{k})|}{P_1(\mathbf{k})}, \quad 0 \leq Q(\mathbf{k}) \leq 1 \tag{23}$$

Its expectation value q which we define with respect to the powerspectral density $P_1(\mathbf{k})$, is given by

$$q := \frac{1}{2\pi}\int d^2\mathbf{k}\, Q(\mathbf{k})P_1(\mathbf{k}) = \frac{1}{2\pi}\int d^2\mathbf{k}\, |P_2(\mathbf{k})|, \tag{24}$$

which provides a suitable index for the average degree of symmetry breaking (we choose the normalization $\int d^2\mathbf{k} P_1(\mathbf{k}) = 2\pi$, consistent with the conventions taken in the next section). For $P_2(\mathbf{k}) = 0$, the case of complete $O(2) \times O(2)$ shift symmetry, the index q vanishes and $a(\mathbf{k})$ and $a(-\mathbf{k})$ are uncorrelated. For $|P_2(\mathbf{k})| = P_1(\mathbf{k})$, where $O(2) \times O(2)$ symmetry is maximally broken, $q = 1$ and the correlations of $a(\mathbf{k})$ and $a(-\mathbf{k})$ are maximal. Now that we determined the general 2-point functions for each of the two symmetry classes we can proceed by choosing specific functions $C_1(r)$, $C_2(r)$ and investigating the properties of typical realizations for the corresponding Gaussian orientation maps.

4 Gaussian orientation maps

Whereas it would be somewhat cumbersome to create realizations of Gaussian orientation maps in x-space, it is quite easy to do this in the Fourier domain, as most of the Fourier modes $a(\mathbf{k})$ decouple, due to translation invariance. In order to inspect the consequences of broken shift-twist symmetry on the map layout we define a set of model correlation functions and then give examples of the resulting patterns.

4.1 How to generate gaussian orientation maps

In this subsection we present a straightforward method for generating realizations of Gaussian orientation maps numerically, given correlation functions $C_1(\mathbf{r})$ and $C_2(\mathbf{r})$, or their Fourier transforms $P_1(\mathbf{k})$ and $P_2(\mathbf{k})$. In the following we assume that Fourier space is discretized, i.e. that all $\mathbf{k}$ vectors are located on a lattice. A realization of a Gaussian map $z(\mathbf{x})$ is then constructed by superposition of complex plane waves $z(\mathbf{x}) = \sum_{\mathbf{k}} a(\mathbf{k}) e^{i\mathbf{k}\mathbf{x}}$, where the amplitudes $a(\mathbf{k})$ are normally distributed, complex valued random numbers satisfying

$$\langle a(\mathbf{k})\bar{a}(\mathbf{k}')\rangle = P_1(\mathbf{k})\,\delta_{\mathbf{k},\mathbf{k}'} \tag{25}$$

$$\langle a(\mathbf{k})a(\mathbf{k}')\rangle = P_2(\mathbf{k})\,\delta_{\mathbf{k},-\mathbf{k}'} \tag{26}$$

Due to its positive definiteness C can be decomposed as follows:

$$\mathsf{C} = \mathsf{V}^T\mathsf{V} \tag{27}$$

with symmetric matrix V

$$\mathsf{V} = \frac{1}{2\,(\sqrt{\lambda 1} + \sqrt{\lambda 2})} \begin{pmatrix} P_1 + 2\sqrt{\lambda_1\lambda_2} & \mathrm{Re}P_2 & 0 & \mathrm{Im}P_2 \\ \mathrm{Re}P_2 & P_1 + 2\sqrt{\lambda_1\lambda_2} & \mathrm{Im}P_2 & 0 \\ 0 & \mathrm{Im}P_2 & P_1 + 2\sqrt{\lambda_1\lambda_2} & -\mathrm{Re}P_2 \\ \mathrm{Im}P_2 & 0 & -\mathrm{Re}P_2 & P_1 + 2\sqrt{\lambda_1\lambda_2} \end{pmatrix}$$

where the argument $\mathbf{k}$ is omitted here and in the following for ease of notation. Given a set of independent, normally distributed, real valued random variables

$$\xi = (\xi_1,\ \xi_2,\ \xi_3,\ \xi_4)$$

of zero mean and unit variance,

$$\langle \xi_i \rangle = 0 \qquad \langle \xi_i \xi_j \rangle = \delta_{ij}$$

The choice of

$$\eta = \mathsf{V}\xi$$

then gives random variables with desired covariance matrix C:

$$\langle \eta_i \eta_j \rangle = \sum_{kl} \mathsf{V}_{ik}\mathsf{V}_{jl}\langle \xi_k \xi_l \rangle = \sum_k \mathsf{V}_{ik}\mathsf{V}_{kj} = \mathsf{C}_{ij}$$

4.2 A specific model

In this section, we investigate the impact of shift-twist symmetry on the layout of orientation maps for realizations of GRFs for a specific set of correlation functions. Optical imaging data reveals that the powerspectrum $P_1(\mathbf{k})$ of OPMs occupies an annulus in two dimensional $\mathbf{k}$-space, organized around a circle of typical wavenumber k_0, which reflects the fact that OPMs are arranged in repetitive hypercolumns of typical spatial scale $\Lambda = \frac{2\pi}{k_0}$ ([15] and references therein). Accordingly, we define a set of functions $P_1(\mathbf{k})$ sharing this property, depending on a parameter β controlling the width of the annulus. For a given value of the order parameter q we further define a model for $P_2(\mathbf{k})$ fullfilling inequality (23).

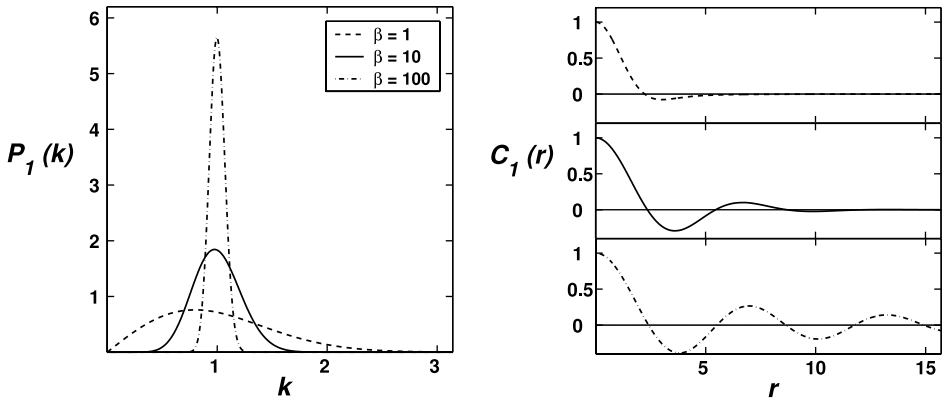

Fig. 3. Model powerspectra $P_1(k)$, width controlled by parameter β, and corresponding correlation functions $C_1(r)$.

4.2.1 $P_1(\mathbf{k})$ and $P_2(\mathbf{k})$

For the correlation functions of the ensembles we chose

$$P_1(\mathbf{k}) = A\,|\mathbf{k}|^{\beta} e^{-|\mathbf{k}|^2 B} \qquad P_2(\mathbf{k}) = q\; P_1(\mathbf{k})\; e^{4i\mathrm{Arg}(k_x+ik_y)} \tag{28}$$

with constants A and B,

$$A = 2\left(\Gamma\left(\frac{2+\beta}{2}\right)\right)^{1+\beta} / \left(\Gamma\left(\frac{1+\beta}{2}\right)\right)^{2+\beta}$$
$$B = \left(\Gamma\left(\frac{2+\beta}{2}\right)\right)^{2} / \left(\Gamma\left(\frac{1+\beta}{2}\right)\right)^{2}.$$

The correlation functions depend on two parameters, β and q, controlling the width of the power spectrum and the amount of symmetry breaking, respectively. With this choice of A and B the correlations P_1 and P_2 satisfy have following properties:

1. The radial part of $P_1(\mathbf{k})$, for which we write $P_1(k)$ in the following, is normalized to 1,

$$\int_0^\infty dk\, P_1(k) = 1 \tag{29}$$

2. $P_1(\mathbf{k})$ is normalized to 2π

$$\int d^2\mathbf{k}\, P_1(\mathbf{k}) = 2\pi,$$

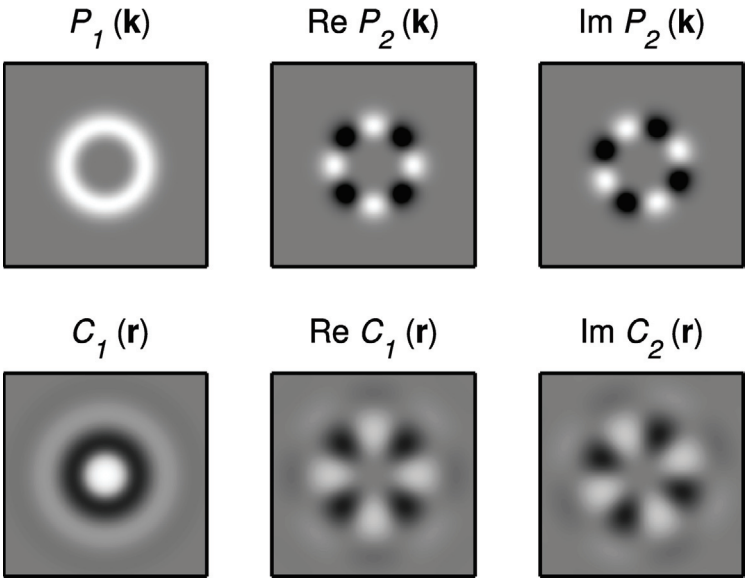

Fig. 4. 2-point correlation function in Fourier representation *(upper row)* and in space representation *(lower row)*. Whereas P_1 and C_1 are real valued, P_2 and C_2 are complex valued and have characteristic cloverleaved shape ($\beta = 10$, $q = 1$).

which, due to rotation symmetry of $P_1(\mathbf{k})$, implies a typical wavenumber $k_0 = 1$,

$$k_0 = \int dk\, k\, P_1(k) = 1. \tag{30}$$

3. $Q(\mathbf{k})$ as defined in Eq. (23) has the same value for all $\mathbf{k}$ and equals q as defined in Eq. (24),

$$|P_2(\mathbf{k})| = q\, P_1(\mathbf{k}).$$

It is thus assumed in this simple model, that the degree of shift symmetry breaking is constant over the relevant range of wavenumbers and spatial scales.

As required by both symmetry classes, the function $P_1(\mathbf{k})$ is rotation invariant. From this follows that $P_2(\mathbf{k})$ is of the form required by Eq. (19) and therefore shift-twist invariant. For $\beta = 1$ the annulus of the powerspectrum is very broad, for large $\beta \gg 1$ it becomes arbitrarily narrow. Only values of $\beta \geq 1$ are considered. Examples of $P_1(\mathbf{k})$ and $P_2(\mathbf{k})$ for different values of β are displayed in Fig. 4.

4.2.2 $C_1(\mathbf{r})$ and $C_2(\mathbf{r})$

The correlation functions in x-space are given by

$$C_1(\mathbf{r}) = {}_1F_1\left(\frac{2+\beta}{2};\ 1\ ; -\frac{\mathbf{r}^2}{4\,B}\right)$$
$$C_2(\mathbf{r}) = (x + i\,y)^4\ {}_1F_1\left(\frac{6+\beta}{2};\ 5\ ; -\frac{\mathbf{r}^2}{4\,B}\right)\ \frac{A\,B^{-\frac{6+\beta}{2}}}{768}$$

where ${}_1F_1$ denotes the confluent hypergeometric function of the first kind (see Appendix A). Indeed, these expressions match the general form of Eqns. (9), (10).

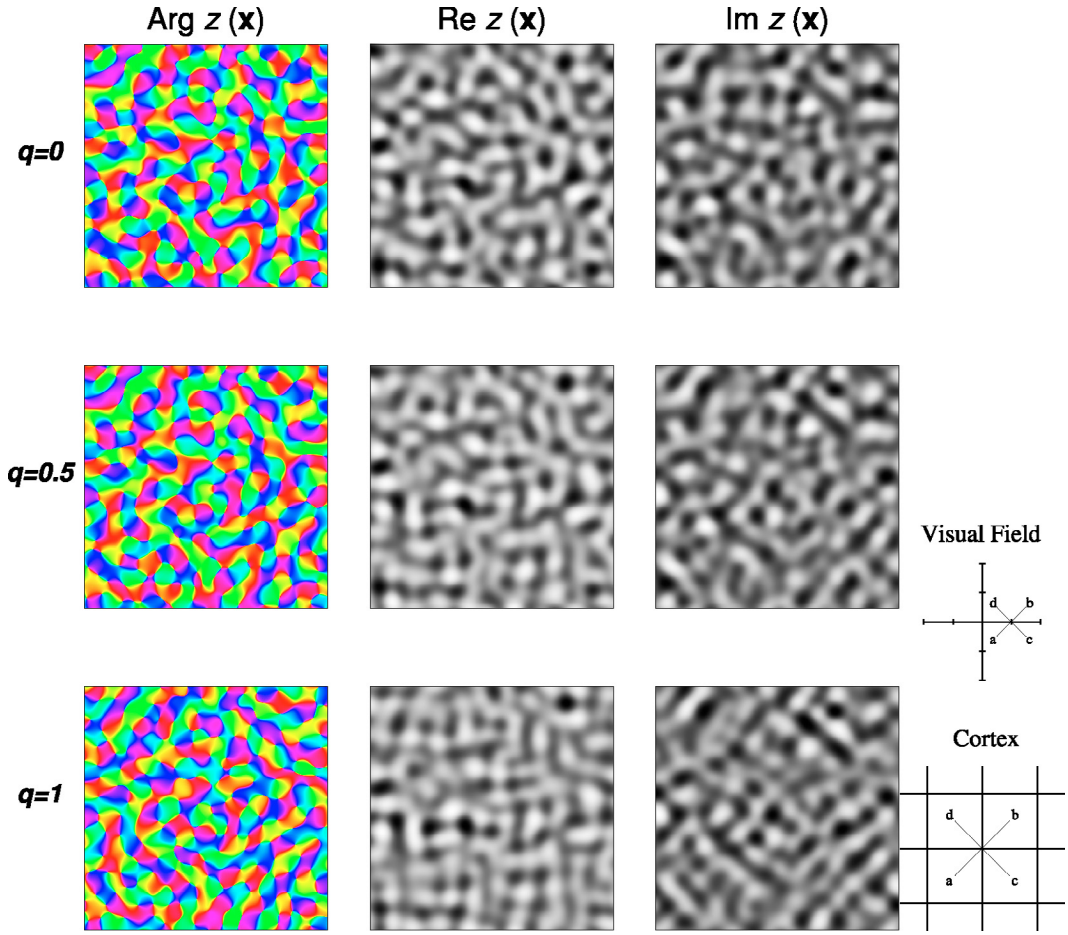

Fig. 5. *Left:* Examples of Gaussian orientation maps, Re$z(\mathbf{x})$ and Im$z(\mathbf{x})$ of a random map for three degrees of broken shift symmetry: $q = 0$, full shift symmetry *(upper row)*; $q = .5$, intermediate case *(middle row)*; $q = 1$, shift symmetry maximally broken *(bottom row)*, $\beta = 10$ for all cases. *Right:* Scheme of the underlying retinotopic map. In our model we identified retinal and cortical coordinates.

4.3 Spatial locking of orientation domains

Figure 5 shows the predicted consequences of increasingly broken shift symmetry on the spatial organization of orientation maps. It displays three examples of random orientation maps generated from ensembles with varying degree of shift symmetry breaking. When shift symmetry in not broken ($q = 0$) the layout of orientation domains preferring cardinal orientations described by the real part of the field $z(\mathbf{x})$ and oblique orientations described by its imaginary part are statistically independent and each exhibits a patchy, irregular and statistically isotropic organization. When shift symmetry is increasingly broken ($q = 0.5, 1$) iso-orientation domains acquire a more band-like appearance and the orientation of the bands becomes spatially locked to specific cortical axes. In the examples shown, cardinal domains are preferentially extending along the horizontal and vertical axes, whereas oblique domains are preferentially extending along the two oblique directions. This spatial locking becomes more pronounced with increasing degree of symmetry breaking.

5 Pinwheel densities

A few years ago, Geisel and Wolf demonstrated that the number of pinwheels generated early in development exhibits a universal minimal value that depends only on general symmetry

properties of the cortical network. This result suggested that in species exhibiting a lower number of pinwheels in the adult, pinwheels must move and annihilate in pairs during the refinement of the cortical circuitry [1]. Verification of this intriguing prediction would therefor provide striking evidence for the activity-dependent generation of the basic visual cortical processing architecture. In this section we revisit the problem of early pinwheel densities for $O(2) \times O(2)$ as well as for shift-twist invariant Gaussian orientation maps and analyze whether broken shift symmetry influences pinwheel generation and affects the previously calculated lower bound.

5.1 Pinwheel densities

Pinwheel centers are the zeros of the complex field $z(\mathbf{r})$, such that at the pinwheel $\mathrm{Re}z = 0$ and $\mathrm{Im}z = 0$. The number $N(A)$ of these zeros in an area A is given by

$$N(A) = \int_A d^2\mathbf{r}\, \delta(\mathrm{Re}z(\mathbf{r}))\delta(\mathrm{Im}z(\mathbf{r})) \left| \frac{\partial[\mathrm{Re}z(\mathbf{r}), \mathrm{Im}z(\mathbf{r})]}{\partial[x,y]} \right| \tag{31}$$

with the Jacobian

$$\frac{\partial[\mathrm{Re}z(\mathbf{r}), \mathrm{Im}z(\mathbf{r})]}{\partial[x,y]} = \frac{\partial \mathrm{Re}z(\mathbf{r})}{\partial x}\frac{\partial \mathrm{Im}z(\mathbf{r})}{\partial x} - \frac{\partial \mathrm{Re}z(\mathbf{r})}{\partial y}\frac{\partial \mathrm{Im}z(\mathbf{r})}{\partial x}.$$

The Jacobian ensures that in the integral of Eq. (31) every pinwheel will increment $N(A)$ by one unit. The expectation value of the number of pinwheel in the ensemble of GRFs is then given by the ensemble average

$$\langle N(A) \rangle = \left\langle \int_A d^2\mathbf{r} \delta(\mathrm{Re}z(\mathbf{r}))\, \delta(\mathrm{Im}z(\mathbf{r})) \left| \frac{\partial[\mathrm{Re}z(\mathbf{r}), \mathrm{Im}z(\mathbf{r})]}{\partial[x,y]} \right| \right\rangle,$$

from which follows that the average pinwheel density $\rho(\mathbf{r})$ equals

$$\rho(\mathbf{r}) = \left\langle \delta(\mathrm{Re}z(\mathbf{r}))\, \delta(\mathrm{Im}z(\mathbf{r})) \left| \frac{\partial[\mathrm{Re}z(\mathbf{r}), \mathrm{Im}z(\mathbf{r})]}{\partial[x,y]} \right| \right\rangle.$$

It is important to note that this expectation value does only depend on local quantities, namely the values of $z(\mathbf{r})$ and its derivatives $\nabla z(\mathbf{r})$ at a given location $\mathbf{r}$. As we assumed translation invariance of the ensemble this value must be the same for all $\mathbf{r}$ and we drop the explicit dependency on $\mathbf{r}$ in the following, writing

$$\rho = \left\langle \delta(\mathrm{Re}z)\, \delta(\mathrm{Im}z) \left| \frac{\partial[\mathrm{Re}z, \mathrm{Im}z]}{\partial[x,y]} \right| \right\rangle.$$

In order to evaluate this expression it is sufficient to know the joint probability density of ∇z. Because any linear functional of a Gaussian random variable is normally distributed, it follows that derivatives ∇z are also normally distributed. For this reason $p(\mathrm{Re}z, \mathrm{Im}z, \nabla\mathrm{Re}z, \nabla\mathrm{Im}z)$ is a multivariate Gaussian of the form

$$p(\boldsymbol{\zeta}) = \sqrt{\frac{\det W}{(2\pi)^6}} \exp\left(-\frac{1}{2} \boldsymbol{\zeta}\, W^{-1}\, \boldsymbol{\zeta} \right)$$

where we used the abbreviation $\boldsymbol{\zeta} = (\mathrm{Re}z, \mathrm{Im}z, \partial_x\mathrm{Re}z, \partial_y\mathrm{Re}z, \partial_x\mathrm{Im}z, \partial_y\mathrm{Im}z)$. The symmetric covariance matrix W is defined by

$$\begin{pmatrix}
\langle \mathrm{Re}z\, \mathrm{Re}z \rangle & \langle \mathrm{Re}z\, \mathrm{Im}z \rangle & \langle \mathrm{Re}z\, \partial_x\mathrm{Re}z \rangle & \langle \mathrm{Re}z\, \partial_y\mathrm{Re}z \rangle & \langle \mathrm{Re}z\, \partial_x\mathrm{Im}z \rangle & \langle \mathrm{Re}z\, \partial_y\mathrm{Im}z \rangle \\
. & \langle \mathrm{Im}z\, \mathrm{Im}z \rangle & \langle \mathrm{Im}z\, \partial_x\mathrm{Re}z \rangle & \langle \mathrm{Im}z\, \partial_y\mathrm{Re}z \rangle & \langle \mathrm{Im}z\, \partial_x\mathrm{Im}z \rangle & \langle \mathrm{Im}z\, \partial_y\mathrm{Im}z \rangle \\
. & . & \langle \partial_x\mathrm{Re}z\, \partial_x\mathrm{Re}z \rangle & \langle \partial_x\mathrm{Re}z\, \partial_y\mathrm{Re}z \rangle & \langle \partial_x\mathrm{Re}z\, \partial_x\mathrm{Im}z \rangle & \langle \partial_x\mathrm{Re}z\, \partial_y\mathrm{Im}z \rangle \\
. & . & . & \langle \partial_y\mathrm{Re}z\, \partial_y\mathrm{Re}z \rangle & \langle \partial_y\mathrm{Re}z\, \partial_x\mathrm{Im}z \rangle & \langle \partial_y\mathrm{Re}z\, \partial_y\mathrm{Im}z \rangle \\
. & . & . & . & \langle \partial_x\mathrm{Im}z\, \partial_x\mathrm{Im}z \rangle & \langle \partial_x\mathrm{Im}z\, \partial_y\mathrm{Im}z \rangle \\
. & . & . & . & . & \langle \partial_y\mathrm{Im}z\, \partial_y\mathrm{Im}z \rangle
\end{pmatrix}$$

where the matrix elements can be expressed in terms of the correlation functions C_1 and C_2 as follows

$$\langle \mathrm{Re}z\,\mathrm{Re}z\rangle = \frac{1}{2}\left[C_1(\mathbf{0}) + \mathrm{Re}C_2(\mathbf{0})\right] \qquad \langle \mathrm{Im}z\,\mathrm{Im}z\rangle = \frac{1}{2}\left[C_1(\mathbf{0}) - \mathrm{Re}C_2(\mathbf{0})\right]$$
$$\langle \mathrm{Re}z\,\mathrm{Im}z\rangle = \frac{1}{2}\mathrm{Im}C_2(\mathbf{0})$$

The remaining matrix elements involving derivatives can be obtained from the previous expressions by differentiation, e.g.

$$\langle \mathrm{Re}z\,\partial_j\mathrm{Re}z\rangle = \frac{1}{2}\partial_j\left[C_1(\mathbf{0}) + \mathrm{Re}C_2(\mathbf{0})\right] \qquad \langle \partial_i\mathrm{Re}z\,\partial_j\mathrm{Re}z\rangle = -\frac{1}{2}\partial_i\partial_j\left[C_1(\mathbf{0}) - \mathrm{Re}C_2(\mathbf{0})\right]$$

Note the occurrence of a minus sign in terms with two derivatives. It is important to realize that due to the prefactor $(x+iy)^4$ occurring in the general formula for $C_2(\mathbf{r})$, Eq. (10), all terms containing C_2, e.g. $C_2(\mathbf{0}), \partial_i C_2(\mathbf{0})$ and $\partial_i\partial_j C_2(\mathbf{0})$ vanish when evaluated at $\mathbf{r} = \mathbf{0}$. For that reason the pinwheel density exclusively depends on the rotation invariant correlation function $C_1$and is in general independent of C_2. This means in particular that the pinwheel density does not depend on the degree of shift symmetry breaking q. The symmetric covariance matrix W then states

$$\mathsf{W} = \frac{1}{2}\begin{pmatrix} C_1(\mathbf{0}) & 0 & \partial_x C_1(\mathbf{0}) & \partial_y C_1(\mathbf{0}) & 0 & 0 \\ . & C_1(\mathbf{0}) & 0 & 0 & \partial_x C_1(\mathbf{0}) & \partial_y C_1(\mathbf{0}) \\ . & . & -\partial_{xx} C_1(\mathbf{0}) & -\partial_{xy} C_1(\mathbf{0}) & 0 & 0 \\ . & . & . & -\partial_{yy} C_1(\mathbf{0}) & 0 & 0 \\ . & . & . & . & -\partial_{xx} C_1(\mathbf{0}) & -\partial_{xy} C_1(\mathbf{0}) \\ . & . & . & . & . & -\partial_{yy} C_1(\mathbf{0}) \end{pmatrix}$$

Due to rotation symmetry also the terms $\partial_i C_1(\mathbf{0})$ and $\partial_i\partial_j C_1(\mathbf{0})$ vanish, and we finally obtain a diagonal matrix

$$\mathsf{W} = \mathrm{diag}(c_A,\ c_A,\ c_G,\ c_G,\ c_G,\ c_G)$$

where we introduced the abbreviations

$$c_A = \frac{1}{2}\,C_1(\mathbf{0}) \qquad c_G = -\frac{1}{4}\,\Delta C_1(\mathbf{0})$$

and used that fact that $\partial_{xx} C_1(\mathbf{0}) = \partial_{yy} C_1(\mathbf{0})$ by rotation invariance of $C_1(\mathbf{r})$. The joint probability distribution $p(\boldsymbol{\zeta})$ then reads

$$p(\boldsymbol{\zeta}) = \frac{1}{(2\pi)^3 c_A c_G^2}\,\exp\left(-\frac{z\bar{z}}{2\,c_A}\right)\exp\left(-\frac{\nabla z \nabla \bar{z}}{2\,c_G}\right)$$

We can now perform the ensemble average, given by the integral

$$\rho = \int d\boldsymbol{\zeta}\, p(\boldsymbol{\zeta})\,\delta(\mathrm{Re}z)\,\delta(\mathrm{Im}z)\left|\frac{\partial[\mathrm{Re}z, \mathrm{Im}z]}{\partial[x,y]}\right|,$$

to obtain the pinwheel density ρ. The result of this straightforward calculation yields (see Appendix B):

$$\rho = -\frac{\Delta C_1(\mathbf{0})}{4\pi C_1(\mathbf{0})} \tag{32}$$

5.2 Model pinwheel densities

Next we evaluate the analytical expression Eq. (32) for ensembles of Gaussian orientation maps defined by the correlation functions Eq. (28). The calculation of the rescaled pinwheel density

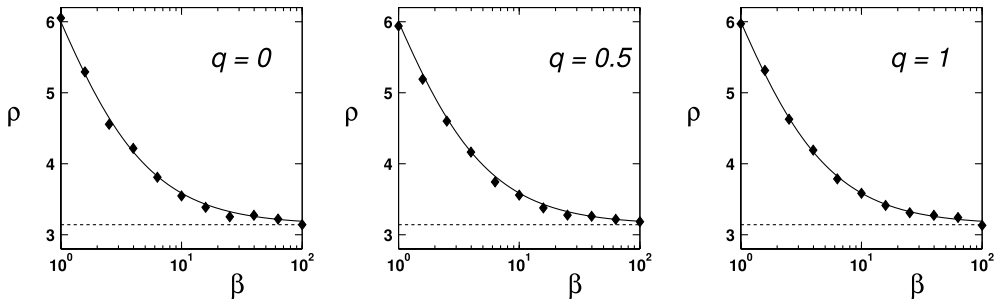

Fig. 6. Relative pinwheel density $\hat{\rho}$ as a function of powerspectral width β for $q = 0$, .5, 1. *Full Line:* Analytical prediction, *Data points:* Numerical simulation, average over 50 GRFs.

$\hat{\rho} = \rho\Lambda^2$ yields

$$\hat{\rho} = \pi \frac{(2+\beta)\Gamma\left[\frac{1+\beta}{2}\right]^2}{2\,\Gamma\left[\frac{2+\beta}{2}\right]^2} \tag{33}$$

which depends on the parameter β controlling the width of the powerspectrum but is independent of q, the degree of shift symmetry breaking. We performed simulations by generating 50 configurations of GRFs for several values of β ($1 \leq \beta \leq 100$]) and for 3 different values of q ($q = 0$, 0.5, 1) in order to check formula (35) and to confirm the prediction that pinwheel densities should be independent of q. For $\beta = 1$, $\hat{\rho} = 6$ and for $\beta \to \infty$, $\hat{\rho} \to \pi$, which is also apparent from Fig. 6. The relative pinwheel density diminishes with decreasing powerspectral width (increasing β) and is asymptotically approaching π from above. As expected, the functional form of $\hat{\rho}(\beta)$ does not depend on the degree of shift symmetry breaking q.

5.3 Lower bound on pinwheel densities

Next we show that relative pinwheel densities of Gaussian orientation maps have an expectation value larger than π. Following the line of arguments given in [1] we switch to Fourier space. First, we express $C_1(\mathbf{0})$ and $\Delta C_1(\mathbf{0})$ as functionals of $P_1(\mathbf{k})$ as follows:

$$C_1(\mathbf{0}) = \frac{1}{2\pi}\int d^2\mathbf{k}\, P_1(\mathbf{k}) \qquad \Delta C_1(\mathbf{0}) = -\frac{1}{2\pi}\int d^2\mathbf{k}\, |\mathbf{k}|^2 P_1(\mathbf{k})$$

The pinwheel density is then given by

$$\rho = \frac{1}{4\pi}\frac{\int d^2\mathbf{k}\, |\mathbf{k}|^2 P_1(\mathbf{k})}{\int d^2\mathbf{k}\, P_1(\mathbf{k})} \tag{34}$$

The exact form of the correlation function $C_1(\mathbf{r})$ or $P_1(\mathbf{k})$, respectively, at the beginning of development is not known. In particular, it is to be expected, that these functions vary from species to species and from individual to individual. The following argument shows that Eq. (34) implies a quantitative estimate of the pinwheel density. For this purpose we define a characteristic wavelength Λ of the pattern by setting $\Lambda = 2\pi/k_0$ with k_0 defined as in section 4, Eq. (30)

$$k_0 = \int dk\, k\, P_1(k),$$

where $P_1(k)$ denotes the radial part of $P_1(\mathbf{k})$, chosen to have norm 1

$$\int dk\, P_1(k) = 1.$$

Rewriting the expression for the pinwheel density as

$$\rho = \frac{\pi}{\Lambda^2} \frac{\int_0^\infty dk\, k^3\, P_1(k)}{\left(\int_0^{2\pi} dk\, k\, P_1(k)\right)^3}.$$

and using Jensen's inequality,

$$\int_0^\infty dk\, k^3\, P_1(k) \geq \left(\int_0^\infty dk\ k\, P_1(k)\right)^3$$

it follows that ρ can be written

$$\rho = \frac{\pi}{\Lambda^2}(1+\alpha) \tag{35}$$

where $\alpha \geq 0$. Thus, the exact form of the power spectral density influences the expected pinwheel density only via the positive definite functional

$$\alpha = 3\int_0^\infty dk\, \frac{(k-k_0)^2}{k_0^2} P_1(k) + \int_0^\infty dk \frac{(k-k_0)^3}{k_0^3} P_1(k) \tag{36}$$

where α is zero, when $P_1(k)$ equals the Dirac delta distribution. The first and the second term are proportional to the variance and skewness of the distribution $P_1(k)$, respectively. From this follows that a Gaussian random pattern of orientation preferences has a minimum pinwheel density,

$$\rho_{\min} = \frac{\pi}{\Lambda^2}$$

independently of the exact form of its spatial correlations. Because two dimensional GRFs are ergodic [38], this lower limit is also valid for the pinwheel density in an individual realization of such a field.

In conclusion, while the pinwheel density depends on the powerspectrum $P_1(\mathbf{k})$ it is independent of $P_2(\mathbf{k})$. As a consequence we conclude that shift-twist symmetry has no effect on the pinwheel density of Gaussian orientation maps. In particular, the previous result concerning the lower bound of the pinwheel density remains unaffected.

6 Conclusion

The formation of OPMs in the visual cortex can be modeled by dynamic field equations [28,35, 37]. Key features of such models crucially depend on the symmetries of the dynamics [1]. Here we introduced a new class of Gaussian random maps which allows to study the consequences of shift-twist symmetry, a fundamental symmetry of visual cortical circuitry [3], on the layout of orientation maps. We use this approach to identify signatures of this new symmetry which are accessible to experimental testing. We also analyzed the consequences of broken shift symmetry for the initial generation of pinwheel defects in orientation preference maps. Because early orientation preference maps are predicted to exhibit Gaussian statistics closed form expressions for early pinwheel densities can be obtained using the theory of Gaussian random fields.

Analyzing these we found that the initial pinwheel density is predicted to be insensitive to the degree of shift symmetry breaking. This implies that even if shift symmetry is broken, defect densities lower than π are predicted to develop through the motion and annihilation of pinwheel pairs. In contradistinction, the breaking of shift symmetry to shift-twist symmetry is predicted to leave clearcut signatures in the spatial layout of cortical orientation maps. These signatures can be quantified by the two point correlation functions of the maps, which are predicted to exhibit a characteristic clover leaf shape. Preliminary evidence suggests that this predicted signature can be directly verified in ensembles of experimentally measured orientation maps from the living visual cortex [39].

7 Appendix A

In this appendix the inverse Fourier transforms of $P_1(\mathbf{k})$ and $P_2(\mathbf{k})$ are calculated.

$$P_1(\mathbf{k}) = A\,|\mathbf{k}|^{\beta} e^{-|\mathbf{k}|^2 B} \qquad P_2(\mathbf{k}) = q\; P_1(\mathbf{k})\; e^{4iArg(k_x+ik_y)} \tag{37}$$

7.1 $P_1(\mathbf{k}) \to C_1(\mathbf{r})$

$$\begin{aligned} C_1(\mathbf{r}) &= \frac{1}{2\pi}\int d^2\mathbf{k}\, e^{(i\,\mathbf{kr})} A\,|\mathbf{k}|^{\beta} e^{-|\mathbf{k}|^2 B} = \frac{A}{2\pi}\int_0^{\infty} dk\, k^{1+\beta} e^{-k^2 B}\int_0^{2\pi} d\phi\, e^{(i\,k\,|\mathbf{r}|\,\cos\phi)} \\ &= A\int_0^{\infty} dk\, k^{1+\beta} e^{-k^2 B} J_0(k\,|\mathbf{r}|) = \frac{1}{2}\,A\,B^{-\frac{2+\beta}{2}}\,\Gamma\left[\frac{2+\beta}{2}\right]\,{}_1F_1\left(\frac{2+\beta}{2};\;1;\;-\frac{\mathbf{r}^2}{4\,B}\right), \end{aligned}$$

where we made use of the formula 6.631 in [40].

$$\int_0^{\infty} dk\, k^{\mu} e^{-k^2 B} J_{\nu}(k\,|\mathbf{r}|) = \frac{|\mathbf{r}|^{\nu}\Gamma[\frac{\nu+\mu+1}{2}]}{2^{\nu+1}B^{\frac{1}{2}(\mu+\nu+1)}\Gamma(\nu+1)}\,{}_1F_1\left(\frac{\nu+\mu+1}{2};\;\nu+1;\;-\frac{|\mathbf{r}|^2}{4\,B}\right), \tag{38}$$

with $\mu = 1+\beta$, $\nu = 0$. From the definition of A and B follows $\frac{1}{2}\,A\,B^{-\frac{2+\beta}{2}}\Gamma[\frac{2+\beta}{2}] = 1$, such that we get

$$C_1(\mathbf{r}) = {}_1F_1\left(\frac{2+\beta}{2};\;1;\;-\frac{|\mathbf{r}|^2}{4\,B}\right)$$

7.2 $P_2(\mathbf{k}) \to C_2(\mathbf{r})$

$$\begin{aligned} C_2(\mathbf{r}) &= \frac{1}{2\pi}\int d^2\mathbf{k}\, e^{(i\,\mathbf{kr})} A\,|\mathbf{k}|^{\beta} e^{-|\mathbf{k}|^2 B} e^{4\,i\,\mathrm{Arg}\mathbf{k}} = \frac{A}{2\pi}\int_0^{\infty} dk\, k^{1+\beta} e^{-k^2 B}\int_0^{2\pi} d\phi\, e^{(i\,k|\mathbf{r}|\,\cos(\phi-\psi_{\mathbf{r}})} e^{4\,i\,\phi} \\ &= \frac{A}{2\pi}\int_0^{\infty} dk\, k^{1+\beta} e^{-k^2 B}\int_0^{2\pi} d\phi\, e^{(i\,k|\mathbf{r}|\,\cos\phi} e^{4\,i\,(\phi+\psi_{\mathbf{r}})}, \end{aligned}$$

where we denote $\psi_{\mathbf{r}} = \mathrm{Arg}\mathbf{r}$. If we use the following expansion (see Abramowitz-Stegun 9.1.44 & 45, p. 361)

$$e^{ik\,|\mathbf{r}|\,\cos\phi} = J_0(k\,|\mathbf{r}|) + 2\sum_{n=1}^{\infty} i^n \cos(n\phi)\, J_n(k\,|\mathbf{r}|),$$

we obtain

$$\begin{aligned} &= A\,e^{4\,i\,\mathrm{Arg}\mathbf{r}}\int_0^{\infty} dk\, k^{1+\beta} e^{-k^2 B}\, J_4(k\,|\mathbf{r}|) = |\mathbf{r}|^4 e^{4\,i\,\mathrm{Arg}\mathbf{r}}\,\frac{A\,B^{-(\frac{6+\beta}{2})}\Gamma[\frac{6+\beta}{2}]}{768}\,{}_1F_1\left(\frac{6+\beta}{2};\;5;\;-\frac{\mathbf{r}^2}{4\,B}\right) \\ &= (x+iy)^4\,\frac{A\,B^{-(\frac{6+\beta}{2})}\Gamma[\frac{6+\beta}{2}]}{768}\,{}_1F_1\left(\frac{6+\beta}{2};\;5;\;-\frac{\mathbf{r}^2}{4\,B}\right) \end{aligned}$$

where, again we made use of Eq. (38), this time with $\mu = 1+\beta$, $\nu = 4$.

8 Appendix B: Pinwheel densities

We first do the integral over Rez and Imz, which collapses due to the delta functions. We are then left with the integral over the gradients. Using the abbreviation

$$R_x = \partial_x \mathrm{Re}z \qquad R_y = \partial_y \mathrm{Re}z \qquad I_x = \partial_x \mathrm{Im}z \qquad I_y = \partial_y \mathrm{Im}z$$

the integral states

$$\rho = \frac{1}{(2\pi)^3 c_A c_G^2} \int dR_x dR_y dI_x dI_y \, |R_x I_y - R_y I_x| \exp\left(-\frac{R_x^2 + R_y^2 + I_x^2 + I_y^2}{2\, c_G}\right)$$

and can be easily evaluated after a coordinate transformation to four dimensional spherical coordinates, given by

$$R_x = g\, \cos\phi\, \cos\theta_1 \qquad R_y = g\, \cos\phi\, \sin\theta_1 \qquad I_x = g\, \sin\phi\, \cos\theta_2 \qquad I_y = g\, \sin\phi\, \sin\theta_2$$

with $0 \le g < \infty,\ 0 \le \phi \le \pi/2,\ 0 \le \theta_1,\ \theta_2 \le 2\pi$ and volume element

$$dR_x dR_y dI_x dI_y = \frac{1}{2}\, g^3 \sin(2\phi)\, dg\, d\phi\, d\theta_1 d\theta_2.$$

The integral in this coordinates is

$$\rho = \int_0^\infty dg\, \frac{g^5}{32\pi^3 c_A c_G^2} \exp\left(-\frac{g^2}{2c_G}\right) \int_0^{2\pi} d\theta_1 \int_0^{2\pi} d\theta_2\, |\sin(\theta_1 - \theta_2)| \int_0^{\pi/2} d\phi\, \sin(2\phi)$$

Integration over the angles yields

$$\rho = \int_0^\infty dg\, \frac{g^5}{16\pi\, c_A c_G^2} \exp\left(-\frac{g^2}{2c_G}\right)$$

Finally, after integrating over the radial component g we get

$$\rho = \frac{1}{2\pi} \frac{c_G}{c_A}$$

We thank M. Kardar, K. Miller, M. Fagiolini, and H. Dinse for inspiring discussions. This research was supported by HFSP, VolkswagenStiftung, and BMBF.

References

1. F. Wolf, T. Geisel, Nature **395**, 73 (1998)
2. W.H. Bosking, Y. Zhang, B. Schofield, D. Fitzpatrick, J. Neurosci. **17**, 2112 (1997)
3. P.C. Bressloff, J.D. Cowan, M. Golubitsky, P.J. Thomas, M.C. Wiener, Philos. Trans. R. Soc. Lond. B. Biol. Sci. **356**, 299 (2001)
4. V. Braitenberg, A. Schüz, *Cortex: statistics and geometry of neuronal connectivity* (Springer, Berlin, 1998)
5. M.B. Luskin, C.J. Shatz, J. Comp. Neurol. **242**, 611 (1985)
6. B.G. Cragg, J. Comp. Neurol. **160**, 147 (1975)
7. N. Daw, *Visual Development* (Plenum Press, New York, 1995)
8. M. Stryker, *Activity-dependent reorganization of afferents in the developing mammalian visual system* (MIT Press, Cambridge, Mass, 1991) Vol. 3, *Proceedings of the Retina Resarch Foundation Symposia*, Chap. 16, p. 267
9. W. Singer, Science **270**, 758 (1995)
10. L.C. Katz, C.J. Shatz, Science **274**, 1133 (1996)

11. D. Maurer, T.L. Lewis, H.P. Brent, A.V. Levin, Science **286**, 108 (1999)
12. A. Antonini, M.P. Stryker, Science **260**, 1819 (1993)
13. J.T. Trachtenberg, M.P. Stryker, J. Neurosci. **21**, 3476 (2001)
14. M.C. Crair, Curr. Opin. Neurobiol. **9**, 88 (1999)
15. M. Kaschube, F. Wolf, T. Geisel, S. Löwel, J. Neurosci. **22**, 7206 (2002)
16. K.D. Miller, E. Erwin, A. Kayser, J. Neurobiol. **41**, 44 (1999)
17. K.D. Miller, J. Neurosci. **14**, 409 (1994)
18. O. Creutzfeldt, *Cortex Cerebri: performance, structural and functional organization of the cortex* (Oxford University Press, 1995)
19. S. LeVay, S. Nelson, *Columnar Organization of the visual cortex* (Macmillan, Houndsmill, 1991), Chap. 11, p. 266
20. D.H. Hubel, T.N. Wiesel, J. Physiol. **160**, 106 (1962)
21. N.V. Swindale, D. Shoham, A. Grinvald, T. Bonhoeffer, M. Hübener, Nat. Neurosci. **3**, 822 (2000)
22. T. Bonhoeffer, A. Grinvald, Nature **353**, 429 (1991)
23. B. Chapman, M.P. Stryker, T. Bonhoeffer, J. Neurosci. **16**, 6443 (1996)
24. M.C. Crair, D.C. Gillespie, M.P. Stryker, Science **279**, 566 (1998)
25. L.E. White, D.M. Coppola, D. Fitzpatrick, Nature **411**, 1049 (2001)
26. J. Sharma, A. Angelucci, M. Sur, Nature **404**, 841 (2000)
27. N.V. Swindale, Proc. R. Soc. Lond. B. Biol. Sci. **208**, 243 (1980)
28. N.V. Swindale, Proc. R. Soc. Lond. B. Biol. Sci. **215**, 211 (1982)
29. N.V. Swindale, Network **7**, 161 (1996)
30. R. Durbin, G. Mitchison, Nature **343**, 644 (1990)
31. Obermayer, Blasdel, Schulten, Phys. Rev. A **45**, 7568 (1992)
32. E. Erwin, K. Obermayer, K. Schulten, Neural. Comput. **7**, 425 (1995)
33. F. Wolf, T. Geisel, Lecture Notes Phys. **527**, 174 (1991)
34. H.Y. Lee, M. Yahyanejad, M. Kardar, Proc. Natl. Acad. Sci. USA **100**, 16036 (2003)
35. F. Wolf, Phys. Rev. Lett. **95**, 208701 (2005)
36. P.C. Bressloff, Biol. Cybern. **93**, 256 (2005)
37. F. Wolf, *Les Houches 2003 Lecture Notes*, in *Methods and Models in Neurophysics* (Elsevier, Amsterdam, 2005)
38. R. Adler, *The Geometry of Random Fields* (Wiley, New York, 1981)
39. M. Schnabel, M. Kaschube, L. White, D. Coppola, S. Löwel, F. Wolf, *Shift-twist Symmetry in natural images and orientation maps*, in *Society for Neuroscience Abstracts* (2005), Vol. 31
40. I.S. Gradshtein, I. Ryzhik, *Table of Integrals, Series, and Products*, 6th edn. (Academic Press, New York, 2000) ISBN 0-12-294760-6